Theoretical predictions of electromagnetic properties of $1g_{9/2}$ odd-neutron nuclei in the Coriolis coupling model

S. L. Heller
Mathematics Department, Staten Island Community College, Staten Island, New York 10301

J. N. Friedman
Physics Department, Western Connecticut State College, Danbury, Connecticut 06810

(Received 9 June 1975)

Magnetic dipole and electric quadrupole moments and reduced transition rates of several $1g_{9/2}$ nuclei are calculated using the wave functions generated in a previous paper. The pattern of wave functions is shown to support the application of a fixed parameter Coriolis coupling model to nuclei in this region. By a total inclusion of both diagonal and nondiagonal single-particle contributions, theoretical magnetic moments for ground and first excited states of both parities are brought into exceptional agreement with experiment. In particular, this analysis resolves the essential equality of $\mu(\frac{7}{2})$ and $\mu(\frac{9}{2})$ in ^{83}Kr as opposed to the expected equivalence of their g factors. Quadrupole moments, calculated without resorting to effective charges, are generally well predicted. Theoretical transition rates are calculated in two instances and agree with experiment.

[NUCLEAR MOMENTS ^{73}Ge, ^{75,77,79,81}Se, ^{83,85}Kr, ^{87}Sr; calculated q, μ. ^{73}Ge; $B(E2)$. ^{83}Kr; $B(M1)$. Deformed Coriolis coupling treatment with pairing. Both parities.]

I. INTRODUCTION

Several experimental studies[1-6] have been made of the electromagnetic properties of the odd-neutron nuclei in the $1g_{9/2}$ shell. Until recently, most workers were treating these nuclei in terms of assumed spherical-vibrational characteristics. In an earlier paper[7] the Coriolis coupling[8] model was applied to obtain the spectra of several of the nuclei in this region. The success in accounting for much of the low energy spectra (both positive and negative parity) with an essentially fixed parameter model strongly supports the interpretation of these nuclei in terms of a rotational statically deformed treatment.

In addition to the weaknesses of the spherical approaches with regard to energy spectra as described in Ref. 7, the following shortcomings pertaining to the electromagnetic properties are evident: (a) Observed static quadrupole moments of the $\frac{9}{2}^+$ ground state of ^{73}Ge and the $\frac{7}{2}^+$ ground state of ^{79}Se are almost 4 and 10 times larger than those expected from the shell model. (b) The magnetic moments for the lowest two positive parity states of ^{83}Kr are expected according to simple (j,j) coupling to be in the ratio of their spins, 9:7, whereas experimentally the moments themselves are about equal.[1,2] (c) Observed $E2$ transitions between low-lying states in this region are enhanced with respect to spherical shell model predictions. For example, the observed $B(E2; \frac{5}{2}-\frac{9}{2})$ of ^{73}Ge and ^{99}Tc are 10 and 30 times, respectively, the calculated single particle transition rates. (d) Whereas ideal vibrational characteristics forbid strong crossover transitions from the two phonon 2^+ state to the ground state, almost all the even Ge, Se, and Kr isotopes possess fairly strong crossover transitions.

In view of (a) the experimental interest in this region, (b) the inability of the spherical approaches to adequately describe the electromagnetic properties, and (c) the comprehensive reproduction of spectral properties throughout the shell presented in Ref. 7, it is the purpose of the present work to extend the investigation of the $1g_{9/2}$ odd-neutron nuclei to obtain the moments of, and the transitions between, the low-lying levels. To this end the strongly coupled nuclear model is further developed to provide expressions for the magnetic and quadrupole moments, and for the reduced transition rates $B(M1)$ and $B(E2)$. No recourse to an effective charge is made. An analysis of the odd-neutron nuclei based on this model is quite successful in predicting the observed magnetic moments and, with one exception, the quadrupole moments. Not much is known of transitions in this region, but here, too, what experimental results are available corroborate well the model predictions.

II. MODEL

As developed in Ref. 7, the Hamiltonian which couples a particle to a deformed rotating multiparticle core is $H = H_R + H_{p-c} + H_p$, where the three

terms represent core rotation, residual interaction of the paired extra-core nucleons, and single particle motion of the last odd nucleon, respectively. The rotational constant for an axially symmetric system A, the quenching factor ξ, and the deformation β are contained within these three terms. In particular, the quenching factor ξ is developed from the effective core overlap parameter

$$\xi_{i-f} = u_i^{(f)} u_f^{(i)} - v_i^{(f)} v_f^{(i)} . \tag{1}$$

The presence of ξ serves to (a) forbid interactions between excited particle and hole (core-excited) states, (b) quench the nondiagonal Coriolis matrix elements, and (c) properly invert the sign of only nondiagonal hole-hole interaction terms.

A Hamiltonian of this nature leads to a total expanded wave function

$$|IM\rangle = \sum_{K,\nu>0} C_{K,\nu} |IMK\nu\rangle_s , \tag{2}$$

where the basis wave functions may be stated as a properly symmetrized product of the D functions $|IKM\nu\rangle$; the deformed single particle functions $\chi_{\Omega,\nu}$; and the intrinsic core functions $\phi_C^{(\Omega,\nu)}$:

$$|IMK\nu\rangle_s = \left[\frac{2I+1}{16\pi^2}\right]^{1/2} [D^I_{MK}(\theta_i)\chi_{\Omega,\nu} + (-)^{I-1/2} D^I_{M-K}(\theta_i)\chi_{-\Omega,\nu}]\, \phi_C^{(\Omega,\nu)} . \tag{3}$$

I, M, and K are the total spin and its projection on the space- and body-fixed axes, respectively, and ν distinguishes between different single particle states with the same $\Omega = j_z$. For a symmetrically deformed nucleus, $k = \Omega$.

The deformed single particle wave functions are expanded in terms of isotropic harmonic oscillator wave functions $|j\Omega\rangle$

$$\begin{aligned} \chi_{\Omega,\nu} &= \sum_j c_{j,\Omega,\nu} |j\Omega\rangle , \\ \chi_{-\Omega,\nu} &= \sum_j (-)^{j-1/2} c_{j,\Omega,\nu} |j-\Omega\rangle , \end{aligned} \tag{4}$$

with expansion coefficients $c_{j,\Omega,\nu}$ as functions of the deformation parameter β.

In the following section, the electric and magnetic properties are derived using the matrix elements of the appropriate multipole operator $\mathfrak{M}(\lambda, \mu)$ evaluated between the states $|IKM\nu\rangle_s$ which involve (a) summations over the expansion coefficients $C_{K,\nu}(\beta)$ and $c_{j,\Omega,\nu}(\beta)$, and (b) the proper core overlap parameter ξ_{i-f}. The μ represents the space-fixed spherical component of the tensor acquired from the body-fixed component according to the transformation $\mathfrak{M}(\lambda, \mu) = \sum_\nu D^\lambda_{\mu,\nu}(\theta_i)\mathfrak{M}'(\lambda, \nu)$.

Moments

The magnetic moment for a single unpaired particle coupled to a surface is

$$\mu = \langle g_s s_z + g_l l_z + g_R R_z \rangle_{M=I} , \tag{5}$$

where g_s, g_l, and g_R are the intrinsic, orbital, and core gyromagnetic ratios and s_z, l_z, and R_z represent z components of the corresponding angular momenta. Since for a strongly coupled system $\bar{R} = \bar{I} - \bar{j}$ and $\bar{j} = \bar{l} + \bar{s}$, the magnetic moment may be separated into core and extra-core particle terms as follows:

$$\mu = {}_s\langle IIK | g_R I_z + G_z | IIK\rangle_s , \tag{6}$$

where G_z is a component of the vector

$$\bar{G} = (g_s - g_l)\bar{s} + (g_l - g_R)\bar{j} \tag{7}$$

and $|IIK\rangle_s$ are expanded according to Eq. (3). The matrix elements of G_z are evaluated by recourse to the spherical tensor nature of G which permits a transformation to intrinsic coordinates. The general form of these matrix elements and the transformation properties of the operator are well known. In terms of single particle operators, the magnetic dipole moment $\mu(I)$ is given by

$$\mu(I) = \mu_c + \mu_0 + 2\mu_+ + \mu_d , \tag{8}$$

which may be regarded as collective, diagonal, nondiagonal, and decoupled contributions to the total matnetic moment, respectively:

$$\mu_c = g_R I , \tag{9a}$$

$$\mu_0 = \frac{1}{(I+1)} \sum_{K,\nu_i,\nu_f} C^{(i)}_{K,\nu_i} C^{(f)}_{K,\nu_f} G_0(K, \nu_i, \nu_f)\xi_{i-f} , \tag{9b}$$

$$\mu_d = \frac{(-)^{I-1/2}(I+\frac{1}{2})}{2(I+1)} \sum_{\nu_i,\nu_f} C^{(i)}_{1/2,\nu_i} C^{(f)}_{1/2,\nu_f} \times G_d(\tfrac{1}{2}, \nu_i, \nu_f) , \tag{9c}$$

$$\mu_+ = \left[\frac{I}{I+1}\right]^{1/2} \sum_{K,\nu_i,\nu_f} C^{(i)}_{K,\nu_i} C^{(f)}_{K,\nu_f} (I1K1|IK+1) \times G_+(K, \nu_i, \nu_f)\xi_{i-f} . \tag{9d}$$

The specific forms of the matrix elements of the general vector $\bar{G}$ are written

$$G_0(K, \nu_i, \nu_f) = (g_s - g_l)\langle s_0\rangle + (g_l - g_R)\langle j_0\rangle , \tag{10a}$$

$$G_\pm(K, \nu_i, \nu_f) = (g_s - g_l)\langle s_\pm\rangle + (g_l - g_R)\langle j_\pm\rangle , \tag{10b}$$

and, in particular for $K = \frac{1}{2}$,

$$G_d(\tfrac{1}{2}, \nu_i, \nu_f) = (g_s - g_l)(-)^l \left[\sum_l a_{l,0,1/2,\nu_i} a_{l,0,1/2,\nu_f}\right] - (g_l - g_R) a_{\nu_i,\nu_f} , \tag{10c}$$

where, as previously defined, a_{ν_i,ν_f} is the generalized decoupling coefficient. Moreover, remembering $K=\Omega$,

$$\langle j_0\rangle = \sum_j \Omega c_{j,\Omega,\nu_i} c_{j,\Omega,\nu_f} \delta(\nu_i,\nu_f), \tag{11a}$$

$$\langle j_+\rangle = \sum_j [(j-\Omega)(j+\Omega+1)]^{1/2} c_{j,\Omega,\nu_i} c_{j,\Omega,\nu_f}, \tag{11b}$$

$$\langle s_0\rangle = \frac{1}{2}\sum_l (a_{l,\Omega-1/2,1/2,\nu_i} a_{l,\Omega-1/2,1/2,\nu_f} - a_{l,\Omega+1/2,-1/2,\nu_i} a_{l,\Omega+1/2,-1/2,\nu_f}), \tag{11c}$$

$$\langle s_+\rangle = \sum_l a_{l,\Omega+1/2,1/2,\nu_i} a_{l,\Omega+1/2,-1/2,\nu_f}, \tag{11d}$$

and the various Nilsson coefficients $a_{l,\Lambda,\Sigma,\nu}$ are related to $c_{j,\Omega,\nu}$ by

$$a_{l,\Lambda,\Sigma,\nu} = \sum_j (l,\tfrac{1}{2},\Lambda,\Sigma|j\Omega) c_{j,\Omega,\nu}, \tag{12}$$

where l is coupled to s ($s=\frac{1}{2}$).

In addition, the raising and lowering forms of G have been usefully connected by

$$G_+(K) = G_-(K+1). \tag{13}$$

The effective residual overlap coefficient ξ, as previously defined in terms of the nature of the states participating in the interaction, varies within the summations which are again taken only over positive half-integral values of K. All the above operators and coefficients are given in terms of initial and final states i and f in preparation for their application in transition rates.

The collective contribution to the static electric quadrupole moment developed along well-known lines of a rotation ellipsoid is

$$Q_{\text{coll}}(I) = Q_0 \sum_{K,\nu} |C_{K,\nu}|^2 \frac{3K^2 - I(I+1)}{(I+1)(2I+1)}, \tag{14}$$

which involves only the diagonal elements of $\mathfrak{M}(2,0)$ between states $|IKK\nu\rangle_s$. Q_0, the intrinsic moment of the core, is given to the second order in β as

$$Q_0 = \frac{3e_p}{\sqrt{5\pi}} ZR^2(\beta + 0.16\beta^2). \tag{15}$$

Due to the diagonal nature of the collective quadrupole operator, the overlap coefficient is unity and therefore does not appear explicitly in the quadrupole expression. Q_{coll} then depends upon ξ only indirectly to the extent that ξ influences the expansion coefficients $C_{K,\nu}$.

Transitions

The reduced λ-multipole transition rate is found from the transition probability according to

$$T(\lambda; i-f) = \frac{8\pi(\lambda+1)}{\lambda[(2\lambda+1)!!]^2\hbar}\left[\frac{E}{\hbar c}\right]^{2\lambda+1} B(\lambda; i-f). \tag{16}$$

According to the techniques described and in terms of the generalized single particle operator G, the explicit form for the $M1$ reduced transition probability is

$$B(M1; i-f) = \frac{3}{4\pi}[B_I + B_0 + B_+ + B_- + B_d]^2, \tag{17}$$

where

$$B_I = g_R[I_i(I_i+1)]^{1/2}\delta(I_i, I_f) \sum_{K,\nu_i,\nu_f} C^i_{K,\nu_i} C^f_{K,\nu_f} \xi_{i-f}, \tag{18a}$$

$$B_0 = \sum_{K,\nu_i,\nu_f} G_0(K,\nu_i,\nu_f)(I_i 1K0|I_f K) C^i_{K,\nu_i} C^f_{K,\nu_f} \xi_{i-f}, \tag{18b}$$

$$B_+ = \frac{1}{\sqrt{2}} \sum_{K,\nu_i,\nu_f} G_+(K,\nu_i,\nu_f)(I_i 1K1|I_f K+1) C^i_{K,\nu_i} C^f_{K+1,\nu_f} \xi_{i-f}, \tag{18c}$$

$$B_- = \frac{1}{\sqrt{2}} \sum_{K,\nu_i,\nu_f} G_-(K,\nu_i,\nu_f)(I_i 1K-1|I_f K-1) C^i_{K,\nu_i} C^f_{K-1,\nu_f} \xi_{i-f}, \tag{18d}$$

$$B_d = \frac{1}{\sqrt{2}} \sum_{\nu_i,\nu_f} G_d(\tfrac{1}{2},\nu_i,\nu_f)(I_i 1\tfrac{1}{2}-1|I_f-\tfrac{1}{2}) C^i_{1/2,\nu_i} C^f_{1/2,\nu_f} \xi_{i-f}. \tag{18e}$$

For odd-neutron nuclei, the $E2$ reduced transition probability is

$$B(E2, i-f) = \frac{5}{16\pi} Q_C, \tag{19}$$

where

$$Q_C = Q_0 \sum_{K,\nu_i,\nu_f} C^i_{K,\nu_i} C^f_{K,\nu_f} (I_i 2K0|I_f K) \xi_{i-f}. \tag{20}$$

The summations are all taken over the positive

TABLE I. Optimized positive parity wave functions.

Nucleus		^{75}Se		^{73}Ge		^{77}Se		^{77}Se		^{79}Se		^{79}Se	
β		0.20		0.19		0.19		−0.28		+0.28		0.28		0.28	
ξ		0.75		0.82		0.82		0.80		0.80		0.78		0.78	
I^π		$\frac{5}{2}^+$		$\frac{9}{2}^+$		$\frac{5}{2}^+$		$\frac{7}{2}^+$		$\frac{7}{2}^+$		$\frac{7}{2}^+$		$\frac{9}{2}^+$	
							$\lvert I, K, \nu \rangle$								
K	ν	$C_{K,\nu}$	$C_{K,\nu}^2$	$C_{K,\nu}$	$C_{K,\nu}^2$	$C_{K,\nu}$	$C_{K,\nu}^2$	$C_{K,\nu}$	$C_{K,\nu}^2$	$C_{K,\nu}$	$C_{K,\nu}^2$	$C_{K,\nu}$	$C_{K,\nu}^2$	$C_{K,\nu}$	$C_{K,\nu}^2$
$\frac{9}{2}$	$\frac{9}{2}$	0.0	0.0	0.0202	0.0004	0.0	0.0	0.0	0.0	0.0	0.0	0.0	0.0	0.1430	0.0205
$\frac{7}{2}$	$\frac{7}{2}$	0.0		0.0003		0.0		0.0125		0.0005		−0.0017		−0.0002	
	$\frac{9}{2}$	0.0	0.0	0.0955	0.0091	0.0	0.0	0.9051	0.8191	−0.2448	0.0600	0.4930	0.2431	0.4342	0.1885
$\frac{5}{2}$	$\frac{5}{2}$	−0.0023		0.0001		−0.0028		0.0386		0.0088		−0.0099		−0.0020	
	$\frac{7}{2}$	0.0008		0.0015		0.0009		−0.0004		−0.0029		0.0007		−0.0008	
	$\frac{9}{2}$	0.1668	0.0278	0.2647	0.0701	0.1816	0.0330	0.3975	0.1580	−0.5984	0.3581	0.7806	0.6093	0.6654	0.4428
$\frac{3}{2}$	$\frac{3}{2}$	0.0003		0.0002		0.0003		0.0002		−0.0007		0.0002		0.0000	
	$\frac{5}{2}$	−0.0082		0.0034		−0.0095		−0.0099		0.0121		0.0328		0.0338	
	$\frac{7}{2}$	0.0031		0.0028		0.0033		0.0023		0.0006		−0.0087		−0.0090	
	$\frac{9}{2}$	0.4732	0.2258	0.5261	0.2768	0.4957	0.2457	0.1417	0.0201	−0.7232	0.5231	−0.3714	0.1379	−0.4626	0.2140
$\frac{1}{2}$	$\frac{1}{2}$	0.0021		0.0007		0.0023		0.0005		−0.0024		−0.0009		−0.0019	
	$\frac{3}{2}$	−0.0004		−0.0004		−0.0005		−0.0001		0.0002		0.0006		0.0008	
	$\frac{5}{2}$	−0.0193		0.0093		−0.0195		0.0037		−0.0335		0.0066		0.0134	
	$\frac{7}{2}$	0.0043		0.0020		0.0045		−0.0001		0.0109		−0.0006		−0.0026	
	$\frac{9}{2}$	0.8636	0.7459	0.8022	0.6435	0.8490	0.7208	0.0325	0.0011	0.2396	0.0574	0.0917	0.0084	0.3644	0.1328

TABLE I *(Continued)*

Nucleus		^{81}Se		^{83}Kr				^{85}Kr			
β		0.19		0.19		0.18		0.18		0.13		0.13	
ξ		0.58		0.58		0.62		0.62		0.70		0.70	
I^π		$\frac{7}{2}^+$		$\frac{9}{2}^+$		$\frac{9}{2}^+$		$\frac{7}{2}^+$		$\frac{9}{2}^+$		$\frac{7}{2}^+$	
		$\lvert I, K, \nu\rangle$											
K	ν	$C_{K,\nu}$	$C_{K,\nu}^2$	$C_{K,\nu}$	$C_{K,\nu}^2$	$C_{K,\nu}$	$C_{K,\nu}^2$	$C_{K,\nu}$	$C_{K,\nu}^2$	$C_{K,\nu}$	$C_{K,\nu}^2$	$C_{K,\nu}$	$C_{K,\nu}^2$
$\frac{9}{2}$	$\frac{9}{2}$	0.0	0.0	−0.7722	0.5964	−0.7923	0.6277	0.0	0.0	0.9472	0.8972	0.0	0.0
$\frac{7}{2}$	$\frac{7}{2}$	0.0037		−0.0009		−0.0012		0.0043		0.0038		0.0	
	$\frac{9}{2}$	−0.9512	0.9049	−0.5946	0.3536	−0.5622	0.3160	−0.9346	0.8735	−0.3027	0.0916	−0.8871	0.7869
$\frac{5}{2}$	$\frac{5}{2}$	−0.0151		−0.0120		−0.0128		−0.0176		0.0001		0.0	
	$\frac{7}{2}$	0.0013		0.0008		0.0006		0.0014		0.0005		0.0	
	$\frac{9}{2}$	0.2972	0.0883	0.2097	0.0440	0.2174	0.0473	0.3388	0.1148	0.0982	0.0096	0.4270	0.1823
$\frac{3}{2}$	$\frac{3}{2}$	0.0001		0.0001		0.0002		0.0002		−0.0000		0.0	
	$\frac{5}{2}$	−0.0021		−0.0018		−0.0022		−0.0028		0.0000		0.0	
	$\frac{7}{2}$	0.0000		−0.0000		−0.0001		0.0000		0.0001		0.0	
	$\frac{9}{2}$	−0.0798	0.0064	−0.0685	0.0047	−0.0812	0.0066	−0.1047	0.0110	−0.0345	0.0012	−0.1708	0.0292
$\frac{1}{2}$	$\frac{1}{2}$	0.0001		0.0001		0.0001		0.0001		−0.0000		0.0	
	$\frac{3}{2}$	−0.0000		−0.0000		−0.0000		−0.0000		−0.0000		0.0	
	$\frac{5}{2}$	−0.0003		−0.0006		−0.0008		−0.0005		0.0000		0.0	
	$\frac{7}{2}$	−0.0001		0.0000		0.0000		−0.0001		0.0000		0.0	
	$\frac{9}{2}$	0.0138	0.0002	0.0353	0.0012	0.0475	0.0023	0.0202	0.0004	0.0184	0.0003	0.0401	0.0016

TABLE II. Optimized negative parity wave functions; ^{77}Se.

		Negative deformation						Positive deformation					
β		−0.28		−0.28		−0.28		+0.28		+0.28		+0.28	
ξ		0.60		0.60		0.60		0.60		0.60		0.60	
I^π		$\frac{1}{2}^-$		$\frac{3}{2}^-$		$\frac{5}{2}^-$		$\frac{1}{2}^-$		$\frac{3}{2}^-$		$\frac{5}{2}^-$	
		$\lvert I, K, \nu\rangle$											
K	ν	$C_{K,\nu}$	$C_{K,\nu}^2$	$C_{K,\nu}$	$C_{K,\nu}^2$	$C_{K,\nu}$	$C_{K,\nu}^2$	$C_{K,\nu}$	$C_{K,\nu}^2$	$C_{K,\nu}$	$C_{K,\nu}^2$	$C_{K,\nu}$	$C_{K,\nu}^2$
$\frac{7}{2}$	$\frac{7}{2}$	0.0	0.0	0.0	0.0	0.0	0.0	0.0	0.0	0.0	0.0	0.0	0.0
$\frac{5}{2}$	$\frac{5}{2}$	0.0	0.0	0.0	0.0	−0.0034	0.0000	0.0	0.0	0.0	0.0	0.0178	0.0003
	$\frac{7}{2}$	0.0	0.0	0.0	0.0	0.0005	0.0000	0.0	0.0	0.0	0.0	0.0005	0.0000
$\frac{3}{2}$	$\frac{3}{2}$	0.0	0.0	−0.0003	0.0000	−0.0074	0.0001	0.0	0.0	0.0360	0.0013	−0.0489	0.0024
	$\frac{5}{2}$	0.0	0.0	0.0565	0.0032	−0.0743	0.0055	0.0	0.0	0.0161	0.0003	−0.0047	0.0000
	$\frac{7}{2}$	0.0	0.0	0.0012	0.0000	−0.0033	0.0000	0.0	0.0	0.0004	0.0000	−0.0016	0.0000
$\frac{1}{2}$	$\frac{1}{2}$	−0.9993	0.9987	0.9937	0.9875	−0.9947	0.9894	−0.9997	0.9994	0.9977	0.9953	−0.0078	0.9956
	$\frac{3}{2}$	−0.0362	0.0013	0.0333	0.0011	−0.0482	0.0023	0.0244	0.0006	−0.0227	0.0005	0.0325	0.0011
	$\frac{5}{2}$	−0.0013	0.0000	0.0905	0.0082	0.0511	0.0026	0.0030	0.0000	−0.0512	0.0026	−0.0254	0.0006
	$\frac{7}{2}$	0.0064	0.0000	−0.0040	0.0000	0.0088	0.0001	0.0024	0.0000	−0.0014	0.0000	0.0034	0.0000

values of K and the same convention described above applies to the interpretation of ξ_{i-f}.

III. DETAILS OF ANALYSIS

The electromagnetic properties are calculated using the energies and wave functions as developed in Ref. 7. This development incorporates standard values of oscillator quanta $\hbar\omega_0 = 41/A^{1/3}$ MeV, nuclear radius $R = 1.2A^{1/3}$ fm, and spin-orbit strength $C = -0.26\hbar\omega_0$. The well-flattening parameter $D_{N=4,3}$ is observed to be $-0.40\hbar\omega_0$, and $-0.05\hbar\omega_0$ for the 15 $N=4$ positive parity and the 10 $N=3$ negative parity basis states, respectively. The rotational constant A and the deformation β are both taken from the assumed rotational properties of the neighboring even-even core. The quenching factor ξ is estimated according to Eq. (1) and the BCS[9] variational parameters u_μ, v_μ, and always lies between $0.6 \leq \xi \leq 0.8$.

In this way the expansion coefficients $c_{j,\Omega,\nu}$ and $C_{K,\nu}$ are generated and applied to obtain the moments of and the transition rates between the significant low-lying states in accordance with the expressions given in the previous section.

With respect to magnetic properties, the following values for gyromagnetic ratios are adhered to for all nuclei, both for moments and transitions: (a) $g_R = Z/A_0$, (b) $g_l = 0$, and (c) $g_s^* = 0.8g_s$. The value for g_R is acquired from the hydrodynamic model[10]; g_s^* is 80% of the free g_s due to the effects of core polarization.[11]

Electric quadrupole calculations are performed without any recourse to effective charge or recoil approximations, i.e. free space values of $e_p = 1$ and $e_N = 0$ are consistently used.

The optimum wave functions used in the following presentation of results are presented in Tables I and II for positive and negative parity states in terms of the Coriolis expansion coefficients $C_{K,\nu}$ and other pertinent parameters.

IV. PRESENTATION AND DISCUSSION OF RESULTS

Wave functions

As expected, the tables of optimum wave functions generally corroborate the Coriolis coupling model classification scheme as synthesized according to available odd-nucleon count beyond the closed shell. For example, the observed similarity of the spectra of ^{73}Ge and ^{75}Se (both with one extra-core neutron) is extended by the similar pattern of the wave functions of the lowest lying $I = \frac{5}{2}^+$ states and again by the $I = \frac{7}{2}^+$ and $\frac{9}{2}^+$ states of ^{81}Se and ^{83}Kr. Any slight differences in the latter are due primarily to a 16 to 25% variation in rotational constants of the even-even cores of these nuclei.[7]

As can be seen from the positive parity wave function coefficients in Table I, low lying states of all nuclei treated consist of contributions almost exclusively of $1g_{9/2}$ parentage ($\nu = \frac{9}{2}$) which would largely obviate the necessity of performing the summation over ν in Eq. (2). However, for higher lying states or those of known $2d_{5/2}$ ($\nu = \frac{5}{2}$) parentage, the entire $N=4$ shell must be employed for all theoretical considerations. For example, (d-p) reactions identify the first $I = \frac{1}{2}^+$ and the second pair of $I = \frac{5}{2}^+, \frac{3}{2}^+$ (inverted due to decoupling) in ^{79}Se reveal admixtures with considerable emphasis on $\nu = \frac{5}{2}$ parentage.

Accordingly, the theoretical expansion coefficients $C_{K,\nu}$ ($\nu = \frac{5}{2}$) for these three states are found

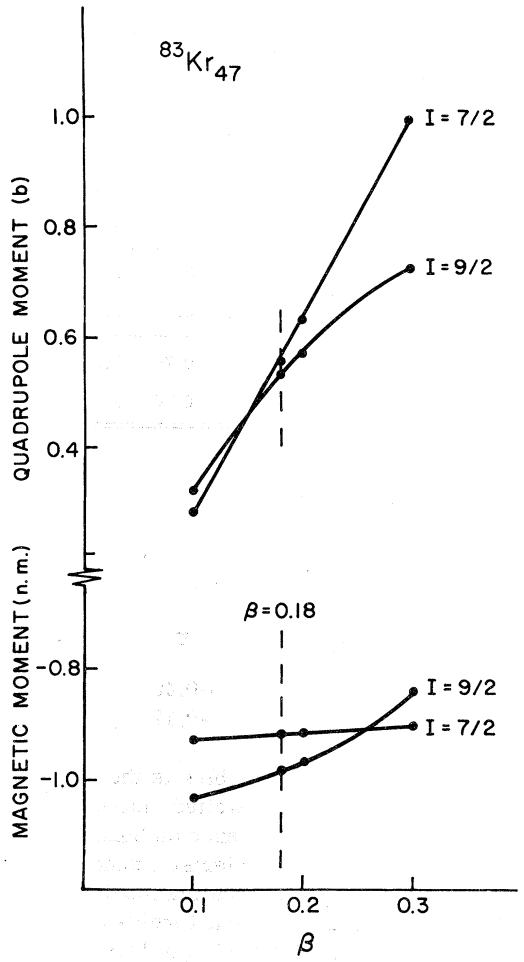

FIG. 1. Variation of magnetic and quadrupole moments of lowest two states of ^{83}Kr vs positive deformation. The quenching factor $\xi = 0.62$. The dotted lines indicate the value of β used to compute the moments of ^{83}Kr given in Tables III and IV.

TABLE III. Magnetic moment (μ_N). All observed values are rounded off to two decimal places.

Nucleus	I^π	β	ξ	μ_R	μ_d	μ_0	μ_+	$\mu(I)$	Obs.	Ref. 23
^{75}Se	$\frac{5}{2}^+$	0.2	0.75	1.133	−1.271	−0.217	−0.546	−1.447		0.77
	$\frac{9}{2}^+$	0.2	0.75	2.040	−1.224	−0.188	−0.692	−0.756		
^{73}Ge	$\frac{9}{2}^+$	0.19	0.80	1.973	−1.141	−0.205	−0.774	−0.922	−0.88	−0.76
	$\frac{5}{2}^+$	0.19	0.80	1.096	−1.205	−0.231	−0.609	−1.558		
^{77}Se	$\frac{1}{2}^-$	0.28	0.60	0.221	−0.015	0.310	0.0	0.515	0.53	0.99
		−0.28	0.60	0.221	0.635	−0.339	0.0	0.517	0.53	0.99
	$\frac{3}{2}^-$	0.28	0.60	0.662	0.023	0.193	−0.003	0.871		
		−0.28	0.60	0.662	−0.834	−0.224	0.004	−0.388		
	$\frac{5}{2}^-$	0.28	0.60	1.104	−0.013	0.127	−0.017	1.185		
		−0.28	0.60	1.104	0.757	−0.135	0.004	1.734		
	$\frac{7}{2}^+$	0.28	0.80	1.545	0.102	−0.797	−0.785	−0.719		
		−0.28	0.80	1.545	0.002	−1.765	−0.335	−0.887		
^{79}Se	$\frac{7}{2}^+$	0.28	0.78	1.506	0.015	−1.304	−0.599	−0.981	−1.02	0.88
	$\frac{9}{2}^+$	0.28	0.78	1.937	−0.234	−0.900	−0.829	−0.855		
^{81}Se	$\frac{7}{2}^+$	0.19	0.58	1.469	0.000	−2.029	−0.162	−0.883		
	$\frac{9}{2}^+$	0.19	0.58	1.889	−0.002	−2.325	−0.249	−0.937		
^{83}Kr	$\frac{9}{2}^+$	0.18	0.62	1.952	−0.004	−2.393	−0.270	−0.986	−0.97	−0.30
	$\frac{7}{2}^+$	0.18	0.62	1.518	0.001	−2.028	−0.206	−0.921	−0.99 [a] −0.94 [b]	−0.23
^{85}Kr	$\frac{9}{2}^+$	0.13	0.70	1.906	−0.001	−2.691	−0.149	−1.084	±1.01 [c]	−0.17
	$\frac{7}{2}^+$	0.13	0.70	1.482	0.003	−1.883	−0.308	−1.013		

[a] Reference 1.
[b] Reference 2.
[c] Reference 3.

to be:

I	$\frac{1}{2}$	$\frac{5}{2}$	$\frac{3}{2}$
$C_{1/2,5/2}$	−0.99	−0.40	+0.93
$C_{3/2,5/2}$	0	−0.12	+0.26

Also apparent from these tables is the constitution of the ground and first excited states fed by $\nu = \frac{9}{2}$ and their strong dependence on bands closely adjacent to the lowest characteristic band for each nuclear class. A specific modification due to the spin projection restriction $I \geq K$ forbids otherwise large contributions in nuclei of spin less than $I = \frac{9}{2}$. In ^{73}Ge the $I = \frac{5}{2}^+$ states possesses no admixtures from $C_{9/2,\,9/2}$, $C_{7/2,\,9/2}$, or $C_{7/2,\,7/2}$ and in ^{83}Kr the $\frac{7}{2}^+$ state is without a $C_{9/2,\,9/2}$ component. In the case of the latter nucleus this selection rule contributes to the excellent electromagnetic predictions associated with this level.

From the negative parity wave function tables presented typically for ^{77}Se (both positive and negative deformations), contributions appear almost exclusively from $C_{1/2,\,1/2}$. This is the result of the effective isolation of the $2p_{1/2}$, $K = \frac{1}{2}$ band from which virtually all negative parity states originate. The dominance of this single coefficient remains essentially unchanged for the lowest lying negative parity states of all $1g_{9/2}$ nuclei throughout a wide range of β encompassing both deformations.

Magnetic and quadrupole moments

All theoretical magnetic moments for ground and first excited states (whenever known) for both parities are in exceptional agreement with experiment. Table III illustrates these results for optimum parameters and provides the contributory

TABLE IV. Quadrupole moment (b). All observed values are rounded off to two decimal places.

Nucleus	I^π	β	ξ	Q_0	Q_{th}	Obs.	Other theories
^{75}Se	$\frac{5}{2}^+$	0.20	0.75	1.320	−0.290	1.0	0.60 [e] 0.30 [f]
	$\frac{9}{2}^+$	0.20	0.75	1.320	−0.423		
^{73}Ge	$\frac{9}{2}^+$	0.19	0.80	1.218	−0.313	−0.28 [a] −0.21 [b]	−0.99 [f]
	$\frac{5}{2}^+$	0.19	0.80	1.218	−0.258		
^{77}Se	$\frac{1}{2}^-$	0.28	0.60	1.905	0.0		
		−0.28	0.60	−1.741	0.0		
	$\frac{3}{2}^-$	0.28	0.60	1.905	−0.380		
		−0.28	0.60	−1.741	−0.346		
	$\frac{5}{2}^-$	0.28	0.60	1.905	−0.543		
		−0.28	0.60	−1.741	0.495		
	$\frac{7}{2}^+$	0.28	0.60	1.905	−0.138		
	$\frac{7}{2}^+$	−0.28	0.60	−1.741	−0.677		
^{79}Se	$\frac{7}{2}^+$	0.28	0.78	1.937	0.239	0.8	
	$\frac{9}{2}^+$	0.28	0.78	1.937	−0.197		
^{81}Se	$\frac{7}{2}^+$	0.19	0.58	1.318	0.563		
	$\frac{9}{2}^+$	0.19	0.58	1.318	0.506		
^{83}Kr	$\frac{9}{2}^+$	0.18	0.62	1.344	0.518	0.27 [c]	0.89 [f]
	$\frac{7}{2}^+$	0.18	0.62	1.344	0.555	0.46 [d]	
^{85}Kr	$\frac{5}{2}^+$	0.13	0.70	0.979	0.494	0.43 [a] 0.45	0.89 [f]
	$\frac{7}{2}^+$	0.13	0.70	0.979	0.365		

[a] See Reference 3.
[b] See Reference 17.
[c] See Reference 18.
[d] See Reference 19.
[e] See Reference 16.
[f] See Reference 23.

terms defined in Eqs. (9a)–(9d). No additional variable parameters are introduced for these calculations; gyromagnetic ratios are fixed for all nuclei as discussed in Sec. III, and are held consistent for transition computations as well. The large generally negative single particle terms μ_0, μ_+, and μ_d significantly reduce the fractional contribution due to the collective μ_R term. Without the inclusion of the nondiagonal contributions μ_d and μ_+, correct magnetic moments are not accurately predicted, again pointing to the importance of the Coriolis interaction. As expected, only class I nuclei experience large decoupling contributions for both parities.

Of particular interest, various researchers employing Mössbauer effect measurements have reported the essential equivalence of $\mu(\frac{7}{2})$ and $\mu(\frac{9}{2})$ in ^{83}Kr as opposed to the expected equivalence of their respective g factors. Pure j-j coupled wave functions cannot explain this anomaly nor account for the forbidden $M1$ transition rate predicted by the shell model. Although retarded, still present configurational admixtures due to residual interaction of a promoted $g_{7/2}$ neutron has accounted for a reduced $\frac{9}{2}^+$ ground state moment.[12] However, if such a technique were applied to the $\frac{7}{2}^+$ excited state, it would not retard the single particle $M1$ transition rate by a factor of 50.

On the other hand, Fig. 1 shows how the $\mu(\frac{7}{2})$ and $\mu(\frac{9}{2})$ moments generated by Coriolis wave functions behave with respect to deformation, approaching one another and crossing over at $\beta \approx 0.25$ without suffering any loss in $M1$ transition

TABLE V. Reduced transition rates.

Nucleus	ΔE (keV)	I_i	I_f	α_T	Multipole	Reduced multipole transition rate B_{th}	B'_{th}	B_{obs}
^{73}Ge	13.5	$\frac{5}{2}^+$	$\frac{9}{2}^+$	679 [b]	$B(E2)$ (b^2)	5.40(−2) [a]	3.68 (1)	2.76 (1)
^{83}Kr	9.3	$\frac{7}{2}^+$	$\frac{9}{2}^+$	11 ± 2 [c]	$B(M1)(\mu_N^2)$	1.80(−2)	2.16(−1)	3.34(−1)

[a] 5.40(−2) to be read 5.40×10^{-2}.
[b] See Reference 4.
[c] See Reference 21.

accuracy.[13] Also presented in a similar manner are the quadrupole moments for the same two spins of ^{83}Kr.

Notwithstanding their large sensitivity to β, the two quadrupole moments are reasonably well predicted and, it is suspected, could be improved with some additional knowledge of the ^{83}Kr positive parity energy levels.

Other ground state quadrupole moments are also well predicted (Table IV), with the exception of ^{79}Se which is about $\frac{1}{3}$ of the unusually large experimental composite value of 0.7–0.9 b. (The corresponding quadrupole moment for ^{83}Kr ($\frac{7}{2}^+$) is only 0.46 b.) Direct quadrupole measurements are difficult and the above values are computed from quadrupole coupling measurements and estimated second electrostatic field derivatives which assume a similar band structure of ^{79}Se and the molecules OCS and OCSe.[14] Measurements of the quadrupole moment of ^{75}Se ($\frac{5}{2}^+$) are in turn directly based upon ^{79}Se; the ratio given[15] is $Q(^{75}\text{Se})/Q(^{79}\text{Se}) = 1.26$, which agrees with the absolute value of this ratio computed from the present model of 1.22. Also, using an essentially similar Coriolis coupling approach for ^{75}Se and relaxing the condition for fixed parameters, Sanderson[16] was able to optimize and better relate his value of $Q = 0.6$ with the available experimental result for ^{75}Se.

It should be noted that large deformations and hence large intrinsic quadrupole moments Q_0 do not lead to large total collective moments. This is due to the form of the projection factor $3K^2 - I(I+1)$, which changes sign (negative to positive) at $K = \frac{7}{2}$ for $I = \frac{9}{2}$ spins and at $K = \frac{5}{2}$ for $I = \frac{5}{2}$ and $\frac{7}{2}$. In this way small or even negative quadrupole moments can be obtained from large intrinsic moments. For example, ^{73}Ge, $I = \frac{9}{2}$, possess a $Q_0 = 1.218$ and wave functions predominantly from $K = \frac{1}{2}$ and $\frac{3}{2}$, i.e. $|C_{1/2,\,9/2}|^2 = 0.6435$, $|C_{3/2,\,9/2}|^2 = 0.2768$ (see Table I). This results in largely negative projections and a total moment of $Q = -0.383$, which compares favorably with the observed $Q = -0.28$.

Electromagnetic transitions

Little is known about positive parity lifetimes of nuclei in this region. Very few $M1$, and one $E2$, low-lying excited to ground state transition rates have been measured. Although recent investigations[6] of higher spin states of ^{73}Ge have resolved numerous ambiguities, no further specific information concerning branching ratios or lifetimes or transition rates between the lower-lying states has been reported. In particular, the spin of the 69 keV state has been confirmed to be $\frac{7}{2}^+$, and the presence of higher $\frac{11}{2}^+$ and $\frac{13}{2}^+$ states has been verified. These measurements are supportive of the present Coriolis-coupling treatment of this nucleus which readily predicts all three of these states. The relatively tight grouping of the low-lying spectrum also corroborates an earlier conclusion of a slightly smaller deformation than the $\beta = 0.19$ given in Ref. 7.

Using the eigenfunctions generated by the model for optimized values of all parameters (see Tables I and II) and the expressions developed in Sec. II, the reduced electromagnetic transition rates for both ^{73}Ge and ^{83}Kr are calculated. The results are given in Table V.

The last column is computed from values of lifetimes given in the *Table of Isotopes*.[20] The next to last column recalculates the theoretical reduced transition rates, taking into account the emission of conversion electrons according to $B' = B(1 + \alpha_T)$. Both internal conversion coefficients are large, especially for the ^{73}Ge transition (see Table V), because of the small differences in energy involved in the respective transitions. Consequently, these corrections play a large role in improving the theoretical transition rates. In both cases the agreement with experimental value is quite good.

Noting further that no effective charges are applied to the $B(E2)$ calculation, the enhancement is seen to be a natural attribute of a deformed theory.

The $B(M1)$ value for ^{83}Kr is the result of sig-

nificant cancellation between the B_+ and B_0 terms of Eq. (17) and consequently the theoretical value for this computation is extremely sensitive to slight changes in the expansion coefficients of the wave function. Thus without significantly altering energy level schemes or other computed observables, the exact experimental value for $B(M2; \frac{7}{2} \rightarrow \frac{9}{2})$ could easily be reproduced.

Summary and conclusions

In view of the systematic reproduction of existing data provided by the present model, the general conclusion of this investigation is that the odd-neutron nuclei in the $1g_{9/2}$ shell may be interpreted in terms of a rotational statically deformed approach. This conclusion is reinforced by the fact that all parameters are established by physical observations which permit a unified set of consistent assumptions to produce a model with no free parameters.

Low energy excitations, including spectral anomalies, and all ground state spins can be well accounted for. Magnetic moments in all cases reveal detailed quantitative agreement. Quadrupole moments, with the single discrepancy of ^{79}Se (which is unaccounted for by any other model and is usually attributed to deformation), are fairly well predicted. Lack of experimental data permits only a limited test of the theory with respect to transition rates, but preliminary results for available data are encouraging. Again it is significant to point out that all quadrupole calculations are performed without the use of effective charges.

Core polarization effects due to extra-core particle interactions with the core usually necessitate effective charge introduction. Such polarization is more naturally inherent in this model which at the outset incorporates a quadrupole surface deformation.

The anticipated patterns of deformation through the shell as suggested by energy spectra and $B(E2)$ transition rates of even-even neighbors are fully corroborated in each case by the Coriolis calculation. Best agreements were always obtained using the values of parameters revealed by adjacent even-even nuclei. Distortions appear uniformly prolate with the exception of ^{77}Se which permits an acceptable explanation for either deformation, the oblate being preferred because of a correctly predicted ground state spin. The magnitude of β, smallest near both shell closures, increases for classes of nuclei more centrally located within the $1g_{9/2}$ subshell.

In conclusion, then, the success of this investigation of moments and transition rates, together with our earlier accurate description of nuclear spectra, indicate that this interpretation of the $1g_{9/2}$ neutron shell joins the $1f_{7/2}$ shell conclusions of Malik and Scholz[22] in suggesting "that a deformed nuclear model may be closer to reality in this part of the nuclear mass table."

[1]M. Greenspan, P. Treves, S. Bukshan, and T. Sounino, Phys. Rev. 178, 1802 (1969).
[2]L. E. Campbell, G. J. Perlow, and M. A. Grace, Phys. Rev. 178, 1728 (1969).
[3]G. H. Fuller and V. W. Cohen, Nucl. Data A5, 433 (1969).
[4]R. S. Hager and E. C. Seltzer, Nucl. Data A4, 1 (1968).
[5]T. Sugimitsu, Nucl. Phys. A224, 199 (1974).
[6]K. Forssten, A. Hasselgren, P. L. Monsen, and A. Nilsson, Phys. Scr. 10, 51 (1974).
[7]S. L. Heller and J. N. Friedman, Phys. Rev. C 10, 1509 (1974).
[8]F. B. Malik and W. Scholz, in *Nuclear Structure*, edited by A. Hossain *et al.* (North-Holland, Amsterdam, 1967), p. 34.
[9]J. Bardeen, L. N. Cooper, and J. R. Schrieffer, Phys. Rev. 10, 1175 (1957).
[10]A. Bohr and B. R. Mottelson, K. Dan. Vidensk. Selsk. Mat.—Fys. Medd. 27, No. 16 (1953).
[11]A. B. Migdal, Nucl. Phys. 75, 441 (1966).
[12]H. Noya, A. Arima, and H. Horie, Prog. Theor. Phys. (Kyoto) Suppl. 8, 33 (1958).
[13]S. L. Heller and J. N. Friedman, Bull. Am. Phys. Soc. 19, 991 (1974).
[14]G. R. Bird and C. H. Townes, Phys. Rev. 94, 1203 (1954).
[15]L. C. Aamodt and P. C. Fletcher, Phys. Rev. 98, 1224 (1955).
[16]N. E. Sanderson, Nucl. Phys. A216, 173 (1973).
[17]L. A. Korostyleva, Opt. Spectrosc. 12, 380 (1962).
[18]W. L. Faust and L. Y. Chiu, Phys. Rev. 129, 1214 (1963).
[19]S. L. Ruby and H. Selig, Phys. Rev. 147, 348 (1966).
[20]C. M. Lederer, J. M. Hollander, and I. Perlman, *Table of Isotopes* (Wiley, New York, 1967), 6th Ed.
[21]S. L. Ruby, Y. Hazoni, and M. Pasternak, Phys. Rev. 129, 826 (1963).
[22]W. Scholz and F. B. Malik, Phys. Rev. 153, 1071 (1967).
[23]L. S. Kisslinger and R. A. Sorensen, Rev. Mod. Phys. 35, 853 (1963).